Translational Oncology
www.transonc.com

Volume 11 Number 4 August 2018 pp. 971–978 971

Differential Sensitivity of Human Hepatocellular Carcinoma Xenografts to an IGF-II Neutralizing Antibody May Involve Activated STAT3

Sameer A. Greenall[*,†,‡], Jacqueline Donoghue[†,‡], Terrance G. Johns[†,‡,§] and Timothy E. Adams[*]

[*]CSIRO Manufacturing, Parkville, VIC 3052, Australia; [†]Oncogenic Signalling Laboratory and Brain Cancer Discovery Collaborative Centre for Cancer Research, Hudson Institute of Medical Research, Clayton, VIC 3168, Australia; [‡]Monash University, Clayton, VIC 3168, Australia; [§]Telethon Kids Institute, Subiaco, WA 6008, Australia

Abstract

Hepatocellular carcinoma (HCC) is highly refractory to current therapeutics used in the clinic. DX-2647, a recombinant human antibody, potently neutralizes the action of insulin-like growth factor-II (IGF-II), a ligand for three cell-surface receptors (IGF-IR, insulin receptor A and B isoforms, and the cation-independent mannose-6-phosphate receptor) which is overexpressed in primary human HCC. DX-2647 impaired the growth of tumor xenografts of the HCC cell line, Hep3B; however, xenografts of the HCC cell line, HepG2, were largely unresponsive to DX-2647 treatment. Analysis of a number of aspects of the IGF signaling axis in both cell lines did not reveal any significant differences between the two. However, while DX-2647 abolished phospho (p)-IGF-IR, p-IR and p-AKT signaling in both cell lines, HepG2 showed high levels of p-STAT3, which was unaffected by DX-2647 treatment and was absent from the Hep3B cell line. The driver of p-STAT3 was found to be a secreted cytokine, and treatment of HepG2 cells with a pan- JAK kinase inhibitor resulted in a loss of p-STAT3. These findings implicate the activation of STAT3 as one pathway that may mediate resistance to IGF-II–targeted therapy in HCC.

Translational Oncology (2018) 11, 971–978

Introduction

The requirement of a functional insulin-like growth factor (IGF) signaling axis for oncogenic transformation in a variety of cellular models [1] has acted as a significant catalyst for the development of therapeutic entities targeting this axis, in particular, the IGF-I receptor (IGF-IR), a cell-surface type I transmembrane tyrosine kinase that binds two functionally related polypeptide ligands, IGF-I and IGF-II. While the antitumor activity of IGF-IR–specific small molecule kinase inhibitors and neutralizing monoclonal antibodies had been demonstrated in human tumor xenograft models, the translation of these findings into successful clinical outcomes has been largely disappointing. Early promising results in phase I trials showing disease stabilization and occasional remission in a number of malignancies have not been supported by significant clinical benefit in phase III trials [2,3].

In humans, IGF-I and IGF-II appear to have overlapping roles in the promotion of both fetal and postnatal somatic growth and development, a conclusion consolidated through the clinicopathological profiles of patients who bear either homozygous deletions in the IGF-I gene [4] or inactivating mutations in the paternally expressed copy of the IGF-II gene [5]. This contrasts with the situation in mice, where IGF-II is viewed primarily as an embryonic growth factor [6], with IGF-I, in concert with growth hormone (GH), playing the major role in the promotion of postnatal growth [7]. A complicating factor for the development of therapeutic entities targeting IGF signaling is the inherent redundancy that is a feature of this axis. Both IGF-I and IGF-II bind the IGF-IR with high affinity, activating a number of intracellular effector pathways [8]. In addition, IGF-II binds with high affinity to an alternatively spliced form of the insulin receptor (IR), IR-A, which is the dominant mitogenic isoform found in human cancers [9]. IGF-II also binds the mannose-6-phosphate receptor, a multifunctional protein that may play a role as a tumor suppressor [10].

Address all correspondence to: Tim Adams, CSIRO Manufacturing, Parkville, VIC 3052, Australia. E-mail: Tim.Adams@csiro.au
Received 13 March 2018; Revised 24 May 2018; Accepted 24 May 2018

1936-5233/18
https://doi.org/10.1016/j.tranon.2018.05.011

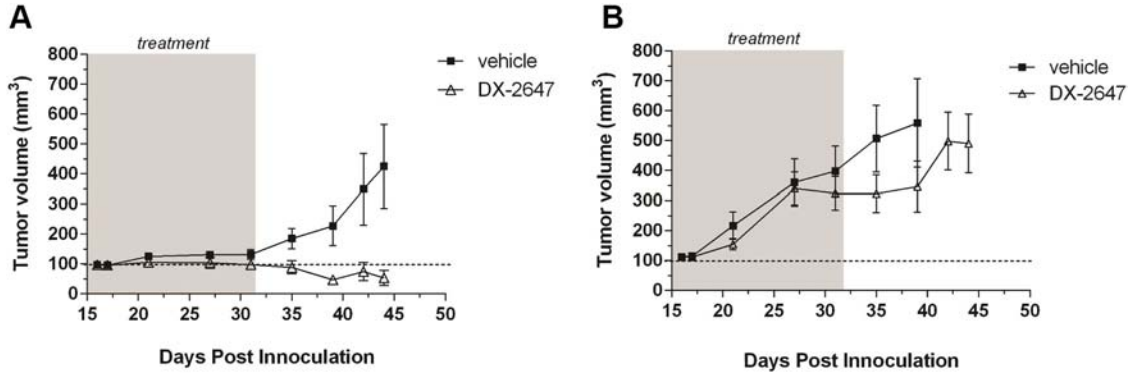

Figure 1. HepG2 cells are resistant to DX-2647 therapy *in vivo*. Hep3B (left panel) and HepG2 (right panel) xenografts were established to 100 mm^3 and treated with vehicle or DX-2647 for 32 days. Data are presented as the mean tumor volume (mm^3) at each time point postinoculation ± S.E.M.

Loss of imprinting of the maternally inherited IGF-II allele, together with reactivation of developmentally regulated promoter elements and the accompanying increase of IGF-II mRNA expression and protein secretion, is a common feature of many childhood and adult cancers [11,12]. Furthermore, stromal-derived IGF-II can facilitate tumor growth by both autocrine and paracrine pathways [13], highlighting the potential of this growth factor as a therapeutic target. We have previously developed DX-2647, a human recombinant monoclonal antibody, as a monotherapy to inhibit the growth of tumor xenografts established using Hep3B cells, a human cell line derived from a hepatocellular carcinoma (HCC [14]). The results are consistent with a number of studies linking deregulated expression of IGF-II with HCC. For example, 15% of patient HCC tissue samples were found to have high levels of IGF-II mRNA expression (>20-2000-fold), together with hypomethylation/transcriptional reactivation of fetal promoter elements, and elevated expression of IR-A [15]. To date, there remains a major unmet need for therapeutic options for the treatment of HCC. In the present study, we have undertaken a detailed analysis of the IGF axis in two well-characterized human HCC cell lines that respond quite differently to the effects of an IGF-II neutralizing antibody when grown as tumor xenografts.

Methods and Materials

Cell Lines

The human HCC cell lines Hep3B and HepG2 were acquired from ATCC-verified stocks at the Victorian Infectious Diseases Reference Laboratories (Melbourne, Australia) and cultured in DMEM containing 10% fetal bovine serum (FBS) and 2.5 mM GlutaMAX (Life Technologies, Carlsbad, CA).

Antibodies and Reagents

The human anti–IGF-II monoclonal antibody (mAb), DX-2647 [14], mouse anti-IR mAb 83-7 [16], and mouse anti–IGF-IR mAb 24-31 [17] were produced in-house at the CSIRO Protein Production Facility. The mouse anti-pan AKT mAb 40D4, rabbit anti-AKT Ser473 mAb D9E, rabbit anti–phospho-ERK1/2 mAb D13.14.4E, mouse anti-ERK1/2 mAb L34F12, rabbit anti-STAT3 mAb 79D7, and mouse anti-STAT3 Tyr705 mAb 3E2 were purchased from Cell Signaling Technology (Danvers, MA). The mouse anti-IR mAb, rabbit anti-IGF-IR polyclonal antibody, monoclonal and polyclonal antibodies against IGFBP-1 to 6, mouse anti-phosphotyrosine mAb pY99, and Protein A/G conjugated to agarose beads were purchased from Santa Cruz Biotechnologies (Santa Cruz, CA). The mouse anti–IGF-II mAb S1F2 was purchased from EMD Millipore (Billerica, MA). Human recombinant IGF-II was purchased from GroPep (Adelaide, SA). The Human Phospho-RTK, Protease and Cytokine Array Kits were purchased from R & D Systems (Minneapolis, MN). The mouse anti-pan actin mAb ACT-05 and the CellTiter Glo cell viability assays were purchased from Thermo Scientific (Waltham, MA) and Promega (Madison, WI), respectively. Swainsonine, kifunensine, and the O-GalNac-transferase inhibitor benzyl 2-acetamido-2-deoxy-α-D-galactopyranoside (OGTi) were purchased from Sigma-Aldrich (St. Louis, MO). CYT-387 and dacomitinib were purchased from SelleckChem (Boston, MA).

Immunoprecipitation and Western Blotting

Cells were washed twice in ice-cold PBS after varying treatments, as indicated, and then lysed in TXC lysis buffer [1% (v/v) Triton X-100, 30 mM HEPES, 150 mM NaCl, 10 mM NaF, 2.5 mM activated $Na3VO_4$ and protease/phosphatase inhibitor cocktails (Thermo Scientific), pH 7.4] for 20 minutes at 4°C. After centrifugation at 21,000×*g* at 4°C for 20 minutes, the protein concentration of the supernatant was determined by bicinchoninic acid assay (Sigma Aldrich), and whole cell lysate (WCL) was subjected to immunoprecipitation (IP) and/or Western blotting. For the IP of IR, 5 μg/ml of the anti-IR antibody 83-7 was added to 400 μg total protein, while for the IP of IGF-IR, 5 μg/ml of the anti-IR antibody 24-31 was added to 400 μg protein. Both antibodies were incubated for 2 hours at 4°C with rotation before the addition of Protein A/G agarose beads overnight at 4°C with rotation. The immunoprecipitates were washed three times in excess TXC buffer and then boiled in 1× reducing LDS sample buffer. For Western blotting, WCL was prepared in either 1× reducing or nonreducing LDS sample buffer. All samples were separated on either 3%-8% Tris-Acetate SDS-PAGE gels or 4%-12% Bis-Tris SDS-PAGE gels, which were then equilibrated before the proteins were transferred to PVDF membranes using the iBlot Dry Blotting system (Life Technologies). Western blotting was performed as previously described [18] using the appropriate primary and secondary antibodies in accordance with the manufacturers' instructions.

Human Phosphorylated Receptor Tyrosine Kinase (RTK), Cytokine, and Protease Detection Arrays

Arrays were performed as per manufacturer's instruction using serum starved cells or supernatants treated with vehicle or 20 μg/ml DX-2647 for 48 hours.

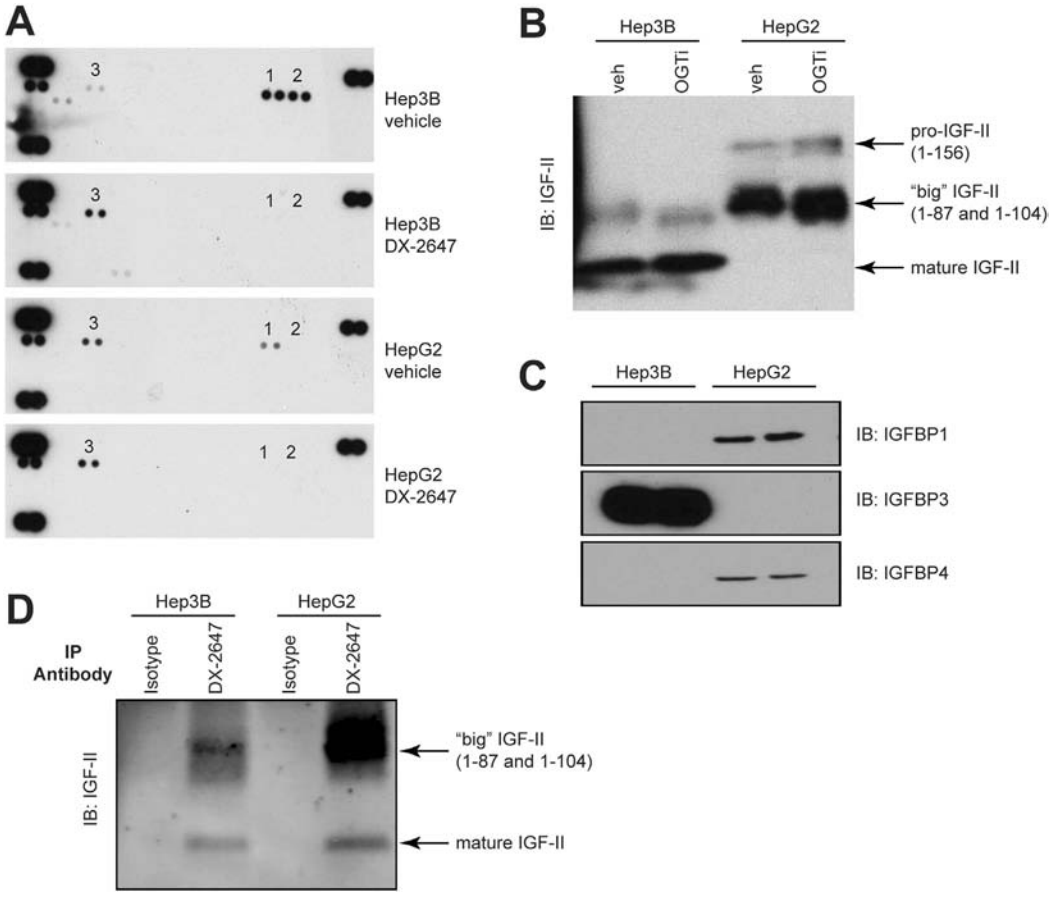

Figure 2. Characterization of the IGF-II axis in Hep3B and HepG2 cells. (A) Cells were treated with vehicle or 20 μg/ml DX-2647 for 48 hours and then tested on activated RTK arrays. Black dots indicate a positive activation signal. (1) p-IR, (2) p-IGF-IR, and (3) p-HER3. Signals in each array corner are positive controls. (B) Western analyses of IGF-II species contained within concentrated and conditioned cell supernatants, treated with vehicle or an O-glycosyltransferase inhibitor (OGTi). IGF-II isoforms are indicated by black arrows. (C) Western analyses of IGFBP expression in cell lysates isolated from Hep3B and HepG2 cells. IGFBP2, IGFBP5, and IGFBP6 were not detected. (D) Immunoprecipitation analysis of bioavailable IGF-II bound from concentrated and conditioned cell supernatants followed by IGF-II blotting. IGF-II species are indicated by black arrows.

Secreted IGF-II and Bioavailable IGF-II Detection Assay

Cells were plated at 5 million per T175 flask overnight. The next day, cells were washed and treated with vehicle, 2 mM of the O-glycosyl-transferase inhibitor 1-benzyl 2-acetamido-2-deoxy-α-D-galactopyranoside (OGTi), or 20 μg/ml DX-2647 for 48 hours in SF-BSA. Supernatants were harvested, centrifuged to remove any cells, and concentrated 60× using 15 ml centrifugal concentrators with a 3 kDa molecular weight cutoff (Millipore). For secreted IGF-II analysis, the concentrated supernatants were subjected to 4%-16% Tricine SDS-PAGE and blotted for IGF-II. For bioavailability tests, the vehicle controls were subjected to IP using either 10 μg/ml of human IgG control (Life Technologies) or DX-2647 for 2 hours at 4°C before addition of Protein A/G agarose beads and overnight incubation at 4°C. IP was washed and analyzed as above for the presence of bioavailable IGF-II which was bound exclusively by DX-2647.

Xenograft Experiments

All experiments were preapproved by the Monash University Animal Ethics Committee. Briefly, 2×10^6 Hep3B or HepG2 cells suspended in a 50:50 mix of cell media and Matrigel were injected into both flanks of female BALB/c *nu/nu* mice. Once tumors reached an average of 80 mm^3, mice were randomly assigned to treatment groups ($n = 6$ per group) and treated with PBS vehicle or 1 mg/kg of DX-2647 twice weekly for 32 days. Tumor volumes were measured as previously described (REF).

Statistics

For measurement of differences in tumor growth after treatments, a Student's t test was employed. All tests were conducted using the GraphPad Prism 6 software. A $P < .05$ value was considered significant.

Results

Response of Human HCC HepG2 Cells to DX-2647 Therapy In Vivo

Our previous *in vitro* data had shown that both human HCC cell lines, Hep3B and HepG2, were highly susceptible to treatment with DX-2647, a human recombinant monoclonal antibody that binds IGF-II with ~20 pM K_D [14]. To determine if the *in vitro* susceptibility of HepG2 cells to DX-2647 treatment could be recapitulated *in vivo*, we conducted animal trials comparing the response of Hep3B and HepG2 tumors to DX-2647 therapy (Figure 1).

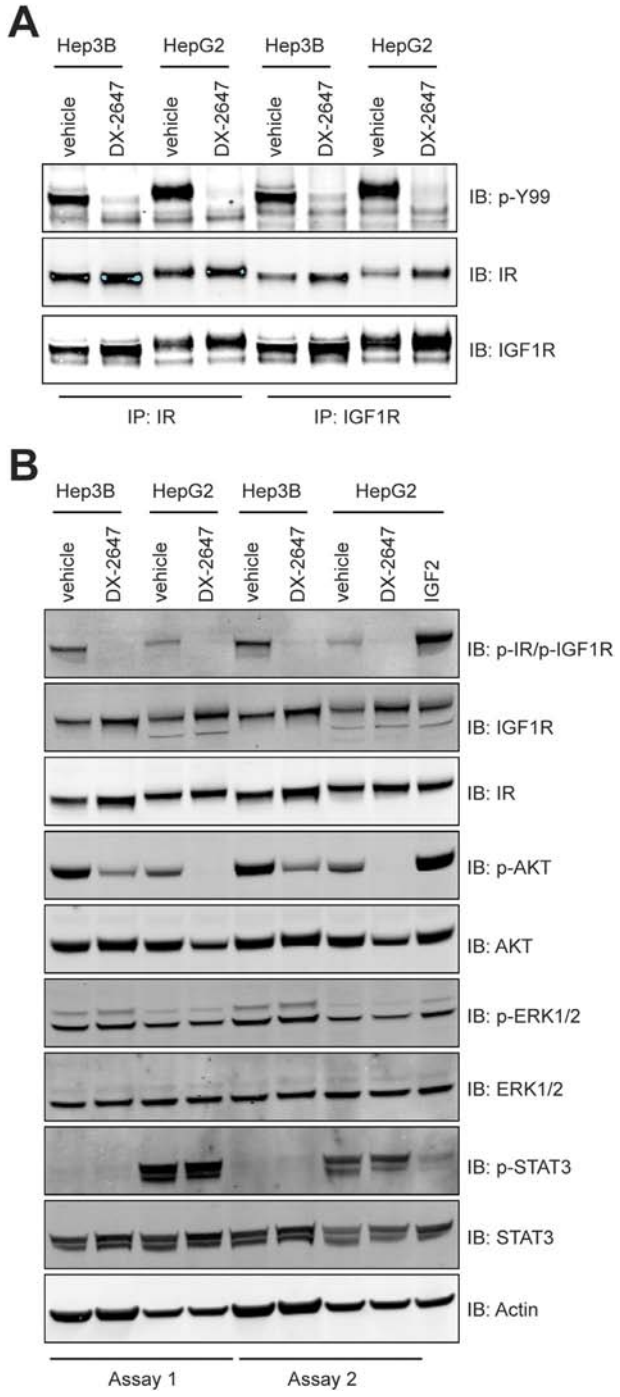

Figure 3. Analysis of IGF-II autocrine signaling in Hep3B and HepG2 cells following DX-2647 treatment. (A) Immunoprecipitation analysis of IR and IGF-IR from cell lysates treated with vehicle or 20 μg/ml DX-2647 for 48 hours followed by blotting for total IR, total IGF-IR, and pan-phosphotyrosine (p-Y99). (B) Western blotting of IR and IGF-IR receptor status and downstream signaling status in cell lysates isolated from Hep3B and HepG2 cells treated with vehicle or 20 μg/ml DX-2647 for 48 hours.

Hep3B tumor growth was significantly impaired by DX-2647 ($P < .001$ from day 35 onward *vs.* vehicle), while the HepG2 tumors were refractory to treatment, with the first indications of initial response appearing much later after initiation of treatment (day 35) but quickly resuming tumor growth at day 42 following cessation of DX-2647 administration. These results demonstrated that the HepG2 tumor cell line, despite being responsive to DX-2647 treatment *in vitro*, was largely unresponsive to treatment *in vivo*.

Secretion of Bioavailable "Big" IGF-II by Hep3B and HepG2 Cells

We used flow cytometry to determine if there were any differences between the cell lines in cell-surface receptor expression of IR and IGF1R, and analyzed receptor glycosylation to see if there were differences in receptor modification. These data show that the IR and IGF-IR were expressed at similar levels (Supplementary Figure 1*A*) but that both receptors were underglycosylated in the Hep3B cell line compared to HepG2 (Supplementary Figure 1*B*).

Previous studies had shown the upregulation of receptor tyrosine kinases (RTK) such as HER3 in response to IGF-IR inhibition [19]. We checked for this by testing vehicle- or DX-2647–treated lysates on activated RTK arrays (Figure 2*A*). Both cell lines showed basal activation of IR, IGF-IR, and HER3. Upon DX-2647 treatment, IR and IGF-IR activation was completely abolished in both cell lines. Both cell lines upregulated activated HER3 in response to DX-2647 treatment.

Western blotting of concentrated samples of conditioned SF medium revealed that Hep3B cells secreted mostly mature IGF-II and a small amount of "big" IGF-II (Figure 2*B*). HepG2 cells secreted both "big" IGF-II and pro–IGF-II, with a small amount of mature IGF-II. In both cell lines, the big and pro–IGF-II forms were O-glycosylated, as treatment with an O-glycosyltransferase inhibitor resulted in a decrease in molecular weight of these species (Figure 2*B*). We then analyzed the concentrated supernatants from both cell lines, grown under normal and hypoxic conditions, for the presence of secreted insulin-like growth factor binding proteins (IGFBPs) (Figure 2*C*); of the six IGFBPs assayed for, only IGFBP-3 was secreted by Hep3B cells, while low amounts of IGFBP-1 and IGFBP-4 were produced by HepG2 cells. There was no difference in the level of secreted IGFBPs following cell growth under hypoxic conditions. To assess the bioavailability of the various IGF-II isoforms, we immunoprecipitated IGF-II from culture supernatants using DX-2647, which only binds uncomplexed (free) IGF-II [14]. Typically, the higher–molecular weight "big" and pro–IGF-II species in both cell lines were the major bioavailable species (Figure 2*D*). Surprisingly, despite the detectable amounts of IGFBP in each cell line (Figure 2*C*), a proportion of bioavailable IGF-II in each cell line was mature IGF-II. Western blotting had indicated that the detected IGFBPs were intact. Analysis of a panel of proteases secreted by each cell line, which can release IGF-II from IGFBP complexes by degradation of IGFBPs [20], demonstrated no significant difference in the species of proteases secreted by each cell line (Supplementary Figure 2), suggesting that differences in IGFBP cleavage were not responsible for IGF-II bioavailability. Collectively, these data suggest show that both cell lines secrete multiple, bioavailable IGF-II species despite the presence of IGFBPs.

DX-2647 Neutralizes p-IR, p-IGF-IR, and p-AKT in Hep3B and HepG2 cells But Fails to Inhibit p-STAT3 Which is Present in HepG2 Only

We next looked to several major intracellular signaling pathways in an attempt to identify differences that might underpin the differential response to antibody therapy observed *in vivo* between the two cell lines. Western blotting of immunoprecipitates from whole cell lysates confirmed that DX-2647 treatment abolished the activation of not only receptor homodimers but also heterodimers of IR and IGF-IR

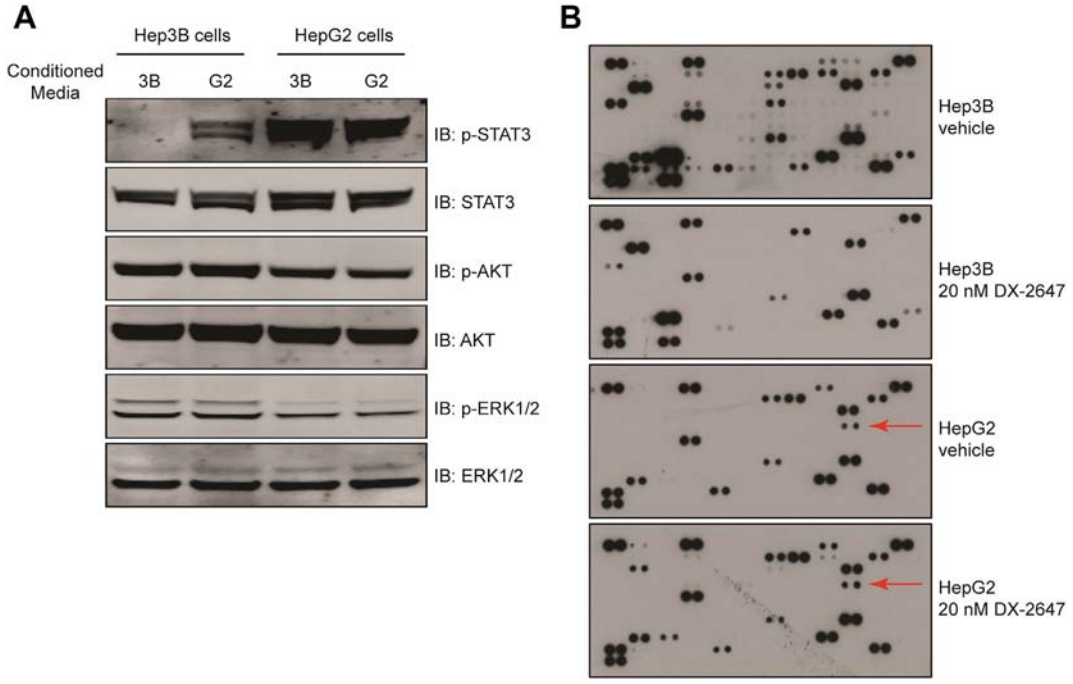

Figure 4. The activator of p-STAT3 in HepG2 is a secreted factor. (A) Western analysis of downstream signaling in Hep3B and HepG2 cells following 45 minutes of reciprocal treatment in conditioned medium. (B) Cytokine array analysis of secreted factors present in Hep3B and HepG2 supernatants after treatment with vehicle or 20 μg/ml DX-2647 for 48 hours. The presence of a black spot indicates presence of a secreted cytokine. The coordinate for the HepG2-unique IL-1ra is indicated by red arrows.

(Figure 3*A*), indicating that the autocrine activation of both receptors in the two HCC cell lines results from the secretion of IGF-II, consistent with results from earlier studies [21] and, in the case of HepG2 cells, possibly IGF-I [22]. Basal levels of p-AKT were higher in Hep3B compared to HepG2; however, DX-2647 potently inhibited p-AKT signaling in both cell lines (Figure 3*B*). Low basal levels of p-ERK1/2 were present in both cell lines and were not inhibited by DX-2647 (Figure 3*B*). The most obvious difference between the two cell lines was in relation to (activated) p-STAT3. In HepG2 cells grown under SF conditions, a strong p-STAT3 signal was observed (Figure 3*B*); in contrast, no corresponding signal was seen in Hep3B cells. Crucially, p-STAT3 was unaffected by treatment with DX-2647. These data suggest that DX-2647 neutralizes the p-IR/p-IGF-IR/p-AKT signaling pathway and that the differences in *in vivo* response observed between cell lines may be linked to the presence of an IR/IGF-IR-independent activation of STAT3.

Active STAT3 in HepG2 Cells is Driven Largely by a Soluble Factor

To establish if the activation of STAT3 in HepG2 cells was in response to a non-IGF autocrine factor, we generated 48-hour conditioned supernatants from Hep3B and HepG2 cell cultures and conducted transfer experiments on the Hep3B cell line to see if HepG2 supernatants could trigger p-STAT3 signaling. Indeed, the addition of HepG2 supernatants to Hep3B cells resulted in the activation of Stat3 (Figure 4*A*) but not when Hep3B-conditioned supernatants were added back to Hep3B cells. This confirmed that at least one component contributing to the appearance of p-STAT3 in HepG2 was a secreted factor.

As our RTK arrays showed no distinct differences between the two cell lines in terms of activated RTK profiles, we concluded that a growth factor was not responsible for driving p-STAT3 in HepG2. Hence, we focused on identifying if the factor was a cytokine or interferon by analyzing conditioned supernatants from each cell line using a human cytokine array (Figure 4*B*). The data from these arrays ruled out interferon gamma (IFN-γ) as a source of p-STAT3 signaling as its signal was not detected on arrays exposed to the supernatants. Additionally, several other factors which classically induce p-STAT3, such as IL-6, IL-11, IL-21, LIF, and MIF, were undetected, demonstrating that the factor was not part of the broader interleukin family (Figure 4*B*). However, the IL-1 receptor antagonist, the induction of which can be driven by a number of cytokines as well as a number of IFNs, was present in HepG2 but not Hep3B supernatants (Figure 4*B*, *arrows*). Treatment with DX-2647 in HepG2 did not alter the global cytokine secretion profile, in contrast to Hep3B which showed a marked reduction in global cytokine output after treatment with DX-2647 (Figure 4*B*).

Active STAT3 Can Be Eliminated by JAK Inhibition in HepG2 Cells

We identified another gp130 cytokine family member, oncostatin-M, as a strong candidate for induction of the p-STAT3 signal observed in HepG2, as Western analyses of conditioned, concentrated supernatants confirmed that oncostatin-M was secreted by HepG2 cells but not by Hep3B cells (Figure 5*A*). However, treatment of HepG2 cells with two separate oncostatin-M neutralizing antibodies (Figure 5, *B* and *C*) failed to prevent STAT3 activation in HepG2 cells. The JAK family of tyrosine kinases plays a key role in the cytokine-mediated activation of the STAT transcription factor protein family. We tested the JAK inhibitor CYT-387 [23] alone and in combination with DX-2647 in HepG2 cells and studied downstream signaling pathways (Figure 5*D*). JAK inhibition strongly reduced p-STAT3 in this cell line, demonstrating that activated STAT3 was JAK-dependent. Treatment with dacomitinib, a pan-HER family antagonist [24], had no effect on p-STAT3 levels (Figure 5*D*). The

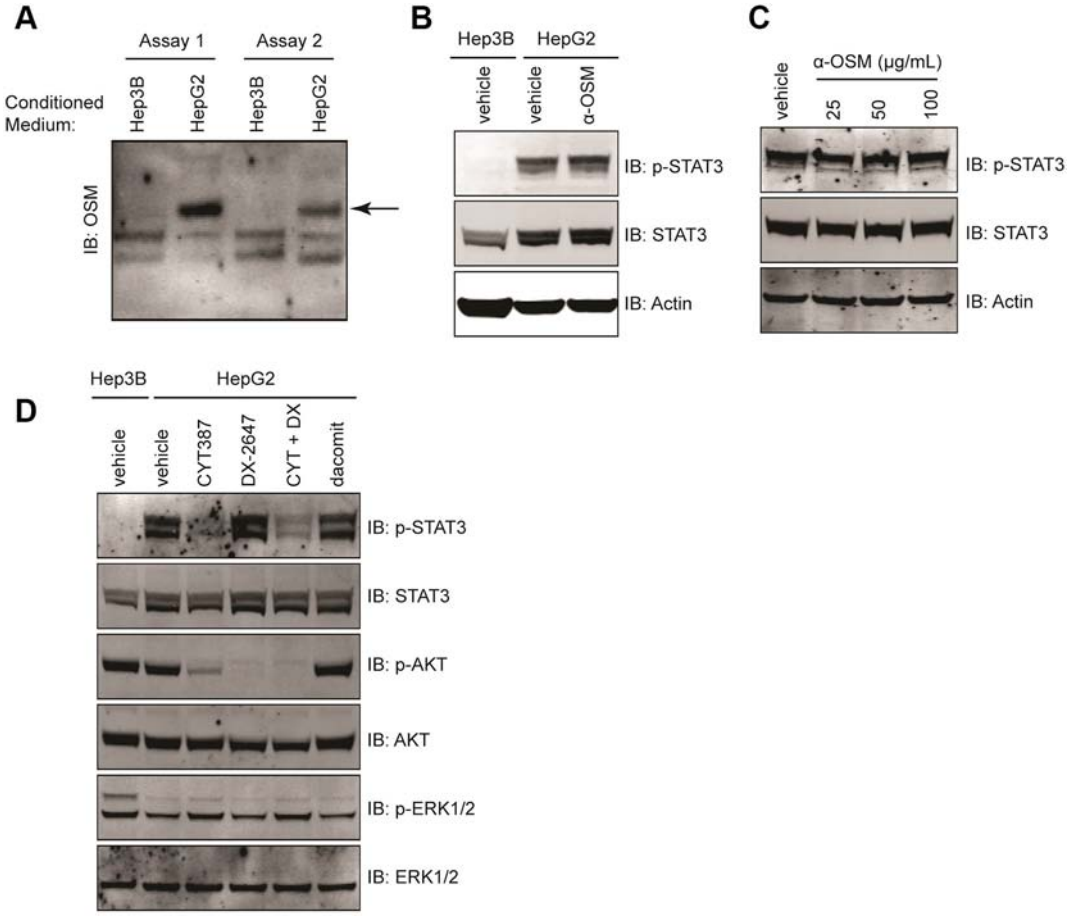

Figure 5. p-STAT3 in HepG2 cells is JAK-dependent. (A) Western analyses for the presence of OSM in concentrated and conditioned cell supernatants. The band corresponding to OSM is indicated by the black arrow. (B-C) Western analyses for p-STAT3 on cell lysates isolated from HepG2 treated with either 50 μg/ml of an Abcam OSM-neutralizing mAb (B) or increasing amounts of a R+D Systems OSM-neutralizing goat polyclonal antibody (C). Actin was included as a loading control. (D) Western analysis of downstream signaling in HepG2 cell lysates isolated following 48-hour treatment with vehicle, 2 μM of CYT-387, 20 μg/ml DX-2647, or a combination of both. A 1 μM dacomitinib–treated control was also included.

combination of CYT-387 and DX-2647 resulted in the inhibition of p-AKT and p-STAT3.

Discussion

The central role played by the autocrine production IGF-II for the growth of Hep3B tumors was originally demonstrated using antisense oligonucleotides and Hep3B orthografts [25]. The sensitivity of Hep3B tumor xenografts to treatment with a dual IG-I/IGF-II-neutralizing mAb has recently been reported elsewhere [15], supporting our earlier findings [14] and those presented in this paper using DX-2647. On the other hand, while DX-2647 effectively ablated the autocrine activation of the IGF-IR/IR axis in HepG2 cells *in vitro*, the growth of HepG2 tumor xenografts was not significantly affected by DX-2647 treatment, indicating that the *in vivo* resistance to DX-2647 is driven by IGF-II–independent signaling.

A key difference between the two cell lines was, under serum-free conditions, the high levels of constitutively active STAT3 in HepG2 cells which were absent in Hep3B cells. The presence of constitutively active STAT3 (p-STAT3) has been observed in 60% of human HCC and is associated with an aggressive phenotype [26]. The activation of STAT3 was largely dependent on Janus-activated kinase(s) (JAKs), as p-STAT3 was inhibited by CYT-387, a potent inhibitor of JAK1 and JAK2 [23], but unaffected by either DX-2647 or dacomitinib, a pan-HER family antagonist [24], ruling out a role for the active EGFR and HER3 observed in our experiments. Cell culture transfer experiments indicated that a soluble factor was, in part, mediating STAT3 activation. Furthermore, at the concentration of DX-2647 used (20 μg/ml *i.e.* >100 nM), we were able to achieve complete neutralization of IGF-IR/IR activation and phosphorylation of AKT, ruling out HepG2-derived, autocrine IGF-I [22] as the STAT3-activating agent, as well as IGF-II. The soluble nature of the factor and the key role played by JAK implicated a member of the gp130 superfamily of cytokines; however, our attempts to identify this unique protein have been unsuccessful despite multiple avenues of interrogation. Figitumumab, a humanized anti–IGF-IR antibody that blocks IGF binding [26], has been shown to inhibit p-STAT3 in HepG2 cells and, like DX-2647, p-AKT [27], but a key difference with our study was their use of 10% serum-containing culture medium. Regardless, tumors xenografts derived from HepG2 have been shown to be potently inhibited by figitumumab [27], possibly by disrupting a ligand-independent IGF-IR–mediated trans-activation of a yet unidentified cell surface receptor which may continue to sustain p-STAT3 after loss of IGF ligand activity. The response of Hep3B xenografts to figitumumab treatment has, to our knowledge, not been reported.

The bioavailability and biological activity of the IGFs are largely regulated by interaction with IGFBPs [28]. Both Hep3B and HepG2 cells secreted a variety of IGF-II isoforms, including partially processed ("big") and mature IGF-II; while mature IGF-II was the dominant isoform produced by Hep3B cells, so-called big IGF-II was the main isoform produced by HepG2 cells. Both cells lines secreted members of the IGFBP family, with appreciable levels of IGFBP-3 being detected in culture supernatants from Hep3B cells (Figure 2*C*). Low levels of IGFBP-1 and -4 were secreted by HepG2 cells, as previously reported [29], although we were unable to reproduce the reported hypoxia-induced secretion of IGFBP-2 in these cells. We established that the majority of the partially-processed isoforms secreted by both Hep3B and HepG2 cells were not complexed with IGFBPs. This was a particularly interesting result in the case of Hep3B cells, where there appeared to be low levels of glycosylated IGF-II and an excess of IGFBP-3; we have previously reported that the glycosylated isoforms of IGF-II bind IGFBP3 and other IGFBPs with similar affinity to mature IGF-II [30]. While we have found that both cell lines secrete a variety of proteases (Supplementary Figure 2), we have seen no evidence that proteolytic degradation of IGFBPs may be a contributing mechanism facilitating the release of bound IGF-II [20].This result implies that there may be other factors operating in the cellular microenvironment to promote the dissociation of glycosylated IGF-II from IGFBPs.

The activation of STAT3 and overexpression of IGF-II have been observed in a significant percentage of human HCC, although the number of tumors that exhibit both characteristics has not been established. As such, the interrelationship between the two pathways in the context of HCC remains unknown, in particular if the presence of activated STAT3 compromises the antitumor efficacy of anti-IGF-II therapy. What in turn drives the constitutive activation of STAT3 in many cases of HCC is largely unknown; our own studies in HepG2 cells point to an as yet unidentified secreted cytokine, but whether this is a common mechanism in HCC is unknown. A better understanding of the interplay between the STAT3 and IGF-II pathways may lead to more effective, biomarker-assisted therapeutic options for a disease where there is a major treatment need.

Supplementary data to this article can be found online at https://doi.org/10.1016/j.tranon.2018.05.011.

Acknowledgments

T. G. J. (GNT1117501) is supported by a fellowship from the National Health and Medical Research Council of Australia. We acknowledge assistance through the Victorian Government's Operational and Infrastructure Support Program.

References

[1] Baserga R, Peruzzi F, and Reiss K (2003). The IGF-1 receptor in cancer biology. *Int J Cancer* **107**, 873–877.

[2] Beckwith H and Yee D (2015). Minireview: were the IGF signaling inhibitors all bad? *Mol Endocrinol* **29**, 1549–1557.

[3] Iams WT and Lovly CM (2015). Molecular pathways: clinical applications and future direction of insulin-like growth factor-1 receptor pathway blockade. *Clin Cancer Res* **21**, 4270–4277.

[4] Woods KA, Camacho-Hubner C, Savage MO, and Clark AJ (1996). Intrauterine growth retardation and postnatal growth failure associated with deletion of the insulin-like growth factor I gene. *N Engl J Med* **335**, 1363–1367.

[5] Begemann M, Zirn B, Santen G, Wirthgen E, Soellner L, Buttel HM, Schweizer R, van Workum W, Binder G, and Eggermann T (2015). Paternally inherited IGF2 mutation and growth restriction. *N Engl J Med* **373**, 349–356.

[6] DeChiara TM, Efstratiadis A, and Robertson EJ (1990). A growth-deficiency phenotype in heterozygous mice carrying an insulin-like growth factor II gene disrupted by targeting. *Nature* **345**, 78–80.

[7] Lupu F, Terwilliger JD, Lee K, Segre GV, and Efstratiadis A (2001). Roles of growth hormone and insulin-like growth factor 1 in mouse postnatal growth. *Dev Biol* **229**, 141–162.

[8] Adams TE, Epa VC, Garrett TP, and Ward CW (2000). Structure and function of the type 1 insulin-like growth factor receptor. *Cell Mol Life Sci* **57**, 1050–1093.

[9] Frasca F, Pandini G, Scalia P, Sciacca L, Mineo R, Costantino A, Goldfine ID, Belfiore A, and Vigneri R (1999). Insulin receptor isoform A, a newly recognized, high-affinity insulin-like growth factor II receptor in fetal and cancer cells. *Mol Cell Biol* **19**, 3278–3288.

[10] Martin-Kleiner I and Gall Troselj K (2010). Mannose-6-phosphate/insulin-like growth factor 2 receptor (M6P/IGF2R) in carcinogenesis. *Cancer Lett* **289**, 11–22.

[11] Breuhahn K and Schirmacher P (2008). Reactivation of the insulin-like growth factor-II signaling pathway in human hepatocellular carcinoma. *World J Gastroenterol* **14**, 1690–1698.

[12] Cui H (2007). Loss of imprinting of IGF2 as an epigenetic marker for the risk of human cancer. *Dis Markers* **23**, 105–112.

[13] Unger C, Kramer N, Unterleuthner D, Scherzer M, Burian A, Rudisch A, Stadler M, Schlederer M, Lenhardt D, and Riedl A, et al (2017). Stromal-derived IGF2 promotes colon cancer progression via paracrine and autocrine mechanisms. *Oncogene* **36**, 5341–5355.

[14] Dransfield DT, Cohen EH, Chang Q, Sparrow LG, Bentley JD, Dolezal O, Xiao X, Peat TS, Newman J, and Pilling PA, et al (2010). A human monoclonal antibody against insulin-like growth factor-II blocks the growth of human hepatocellular carcinoma cell lines in vitro and in vivo. *Mol Cancer Ther* **9**, 1809–1819.

[15] Martinez-Quetglas I, Pinyol R, Dauch D, Torrecilla S, Tovar V, Moeini A, Alsinet C, Portela A, Rodriguez-Carunchio L, and Sole M, et al (2016). IGF2 is up-regulated by epigenetic mechanisms in hepatocellular carcinomas and is an actionable oncogene product in experimental models. *Gastroenterology* **151**, 1192–1205.

[16] Soos MA, O'Brien RM, Brindle NP, Stigter JM, Okamoto AK, Whittaker J, and Siddle K (1989). Monoclonal antibodies to the insulin receptor mimic metabolic effects of insulin but do not stimulate receptor autophosphorylation in transfected NIH 3T3 fibroblasts. *Proc Natl Acad Sci U S A* **86**, 5217–5221.

[17] Soos MA, Field CE, Lammers R, Ullrich A, Zhang B, Roth RA, Andersen AS, Kjeldsen T, and Siddle K (1992). A panel of monoclonal antibodies for the type I insulin-like growth factor receptor. Epitope mapping, effects on ligand binding, and biological activity. *J Biol Chem* **267**, 12955–12963.

[18] Greenall SA, Donoghue JF, Gottardo NG, Johns TG, and Adams TE (2015). Glioma-specific Domain IV EGFR cysteine mutations promote ligand-induced covalent receptor dimerization and display enhanced sensitivity to dacomitinib in vivo. *Oncogene* **34**, 1658–1666.

[19] Desbois-Mouthon C, Baron A, Blivet-Van Eggelpoel MJ, Fartoux L, Venot C, Bladt F, Housset C, and Rosmorduc O (2009). Insulin-like growth factor-1 receptor inhibition induces a resistance mechanism via the epidermal growth factor receptor/HER3/AKT signaling pathway: rational basis for cotargeting insulin-like growth factor-1 receptor and epidermal growth factor receptor in hepatocellular carcinoma. *Clin Cancer Res* **15**, 5445–5456.

[20] Nakamura M, Miyamoto S, Maeda H, Ishii G, Hasebe T, Chiba T, Asaka M, and Ochiai A (2005). Matrix metalloproteinase-7 degrades all insulin-like growth factor binding proteins and facilitates insulin-like growth factor bioavailability. *Biochem Biophys Res Commun* **333**, 1011–1016.

[21] Lund P, Schubert D, Niketeghad F, and Schirmacher P (2004). Autocrine inhibition of chemotherapy response in human liver tumor cells by insulin-like growth factor-II. *Cancer Lett* **206**, 85–96.

[22] Tsai TF, Yauk YK, Chou CK, Ting LP, Chang C, Hu CP, Han SH, and Su TS (1988). Evidence of autocrine regulation in human hepatoma cell lines. *Biochem Biophys Res Commun* **153**, 39–45.

[23] Burns CJ, Bourke DG, Andrau L, Bu X, Charman SA, Donohue AC, Fantino E, Farrugia M, Feutrill JT, and Joffe M, et al (2009). Phenylaminopyrimidines as inhibitors of Janus kinases (JAKs). *Bioorg Med Chem Lett* **19**, 5887–5892.

[24] Engelman JA, Zejnullahu K, Gale CM, Lifshits E, Gonzales AJ, Shimamura T, Zhao F, Vincent PW, Naumov GN, and Bradner JE, et al (2007). PF00299804, an irreversible pan-ERBB inhibitor, is effective in lung cancer models with EGFR and ERBB2 mutations that are resistant to gefitinib. *Cancer Res* **67**, 11924–11932.

[25] Yao X, Hu JF, Daniels M, Shiran H, Zhou X, Yan H, Lu H, Zeng Z, Wang Q, and Li T, et al (2003). A methylated oligonucleotide inhibits IGF2 expression and enhances survival in a model of hepatocellular carcinoma. *J Clin Invest* **111**, 265–273.

[26] He G, Yu GY, Temkin V, Ogata H, Kuntzen C, Sakurai T, Sieghart W, Peck-Radosavljevic M, Leffert HL, and Karin M (2010). Hepatocyte IKKbeta/NF-kappaB inhibits tumor promotion and progression by preventing oxidative stress-driven STAT3 activation. *Cancer Cell* **17**, 286–297.

[27] Kim JG, Kang MJ, Yoon YK, Kim HP, Park J, Song SH, Han SW, Park JW, Kang GH, and Kang KW, et al (2012). Heterodimerization of glycosylated insulin-like growth factor-1 receptors and insulin receptors in cancer cells sensitive to anti-IGF1R antibody. *PLoS One* **7**e33322.

[28] Rajaram S, Baylink DJ, and Mohan S (1997). Insulin-like growth factor-binding proteins in serum and other biological fluids: regulation and functions. *Endocr Rev* **18**, 801–831.

[29] Tazuke SI, Mazure NM, Sugawara J, Carland G, Faessen GH, Suen LF, Irwin JC, Powell DR, Giaccia AJ, and Giudice LC (1998). Hypoxia stimulates insulin-like growth factor binding protein 1 (IGFBP-1) gene expression in HepG2 cells: a possible model for IGFBP-1 expression in fetal hypoxia. *Proc Natl Acad Sci U S A* **95**, 10188–10193.

[30] Greenall SA, Bentley JD, Pearce LA, Scoble JA, Sparrow LG, Bartone NA, Xiao X, Baxter RC, Cosgrove LJ, and Adams TE (2013). Biochemical characterization of individual human glycosylated pro-insulin-like growth factor (IGF)-II and big-IGF-II isoforms associated with cancer. *J Biol Chem* **288**, 59–68.